Different transmitter transients underlie presynaptic cell type specificity of $GABA_{A,slow}$ and $GABA_{A,fast}$

János Szabadics*†, Gábor Tamás†, and Ivan Soltesz*‡

*Department of Anatomy and Neurobiology, University of California, 193 Irvine Hall, Irvine, CA 92697; and †HAS Research Group for Cortical Microcircuits, Department of Comparative Physiology, University of Szeged, Kozep fasor 52, H-6726, Szeged, Hungary

Communicated by Edward G. Jones, University of California, Davis, CA, August 1, 2007 (received for review April 15, 2007)

Phasic (synaptic) and tonic (extrasynaptic) inhibition represent the two most fundamental forms of $GABA_A$ receptor-mediated transmission. Inhibitory postsynaptic currents (IPSCs) generated by $GABA_A$ receptors are typically extremely rapid synaptic events that do not last beyond a few milliseconds. Although unusually slow $GABA_A$ IPSCs, lasting for tens of milliseconds, have been observed in recordings of spontaneous events, their origin and mechanisms are not known. We show that neocortical $GABA_{A,slow}$ IPSCs originate from a specialized interneuron called neurogliaform cells. Compared with classical $GABA_{A,fast}$ IPSCs evoked by basket cells, single spikes in neurogliaform cells evoke extraordinarily prolonged $GABA_A$ responses that display tight regulation by transporters, low peak GABA concentration, unusual benzodiazepine modulation, and spillover. These results reveal a form of $GABA_A$ receptor mediated communication by a dedicated cell type that produces slow ionotropic responses with properties intermediate between phasic and tonic inhibition.

inhibition | neocortex | neurogliaform cell

Ionotropic $GABA_A$ receptors mediate two major types of signaling referred to as phasic and tonic inhibition (1–4). Phasic inhibition mediates the classical, synaptic forms of interactions between a presynaptic GABAergic interneuron and postsynaptic target cells. Phasic GABAergic signals are typically generated rapidly (often with submillisecond rise times) within synapses, whereas low-affinity $GABA_A$ receptors are activated in a transient manner by GABA (5). In contrast, tonic inhibition is a less temporally and spatially precise form of GABAergic inhibition, generated by GABA activating high-affinity, nondesensitizing, mostly extrasynaptic $GABA_A$ receptors (2, 6, 7). Despite its less temporally and spatially focused nature, tonic inhibition is increasingly being recognized to serve critically important, diverse functions in neuronal circuits (8, 9).

Interestingly, a third form of postsynaptic $GABA_A$ receptor-mediated inhibitory response that displays characteristics intermediate between phasic and tonic inhibition (10–13) may also exist. These events have been named $GABA_{A,slow}$ inhibitory postsynaptic currents (IPSCs). In contrast to the more classical, phasic $GABA_{A,fast}$ IPSCs, $GABA_{A,slow}$ IPSCs have almost an order of magnitude slower rise- and decay kinetics (10), are highly sensitive to blockade of GABA uptake (12, 14) and are modulated differently by benzodiazepine agonists (13). Although previous studies indicated that $GABA_{A,slow}$ inputs may be localized on the dendrites of CA1 pyramidal cells, it appears that dendritic filtering alone may not fully explain the slow kinetics (10–12). Moreover, it was suggested that transmitter spillover may contribute to the $GABA_{A,slow}$ IPSCs in contrast to the classical $GABA_{A,fast}$ IPSCs that are thought to be largely limited to the activation of synaptic receptors (5, 10, 14).

Because $GABA_{A,slow}$ IPSCs have been recorded only as spontaneous and extracellular stimulation-evoked events, the cellular sources and the underlying mechanisms of $GABA_{A,slow}$ have not been identified. In a previous study (15), we focused on the ability of neurogliaform cells (NGFCs) to evoke metabotropic, and thus slow, $GABA_B$ receptor-mediated postsynaptic responses. During these experiments, we serendipitously noticed that the rising phase of the $GABA_A$ component of the compound ($GABA_A$ and $GABA_B$) IPSCs generated by NGFCs appeared to be remarkably prolonged. Could there be a connection between the NGFC–$IPSC_A$s and the $GABA_{A,slow}$ events? Building on these clues, in this study, we tested the specific hypothesis that the NGFC-evoked unitary $GABA_A$ receptor mediated responses (NGFC–$IPSC_A$) share the key properties of the $GABA_{A,slow}$ events previously described based on analysis of spontaneous and electrical stimulation-elicited IPSCs. We used paired recordings of identified neocortical interneurons and pyramidal cells to probe the mechanisms of NGFC–$IPSC_A$s, and compared their properties with the fast spiking basket cell (FSBC)-evoked unitary $GABA_A$ IPSCs (FSBC–$IPSC_A$) that are thought to represent $GABA_{A,fast}$ events (5, 12, 14). Our results demonstrate that NGFCs are the sources of $GABA_{A,slow}$ IPSCs in the neocortex and that these extraordinarily prolonged neocortical ionotropic $GABA_A$ responses are generated by a GABA transient with highly unusual characteristics.

Results

NGFCs Generate Slow $GABA_A$ Postsynaptic Responses. All data in this article were obtained by using paired whole-cell patch-clamp recordings from presynaptic NGFCs or FSBCs [supporting information (SI) Fig. 7; Fig. 1*C*] and layer 2/3 postsynaptic pyramidal cells (PCs) (held at −75 mV) in the presence of NMDA, AMPA/kainate and $GABA_B$ receptor blockers (except when noted otherwise). The NGFC–$IPSC_A$s showed dramatically slower rise and decay kinetics compared with the rapid responses elicited by the FSBCs (Fig. 1 *A–D*) (10–90% rise times: NGFC: 4.17 ± 0.24 ms, $n = 71$; FSBC: 0.53 ± 0.02 ms, $n = 40$; weighted decay time constants (τ_D): NGFC: 36.5 ± 1.3 ms; FSBC: 6.4 ± 0.33 ms). However, the IPSC amplitudes were not significantly different (NGFC: 78.6 ± 6.3 pA; FSBC: 106.8 ± 16.3 pA). Because of the uniquely slow kinetics, the charge transfer of the responses elicited by NGFCs was markedly larger than the charger transfer carried by the FSBC–$IPSC_A$s (NGFC: 3284 ± 369 pA·ms; FSBC: 833 ± 136 pA·ms).

Single action potential-evoked NGFC–$IPSC_A$s displayed a significantly smaller trial-to-trial variance in their peak amplitude compared with FSBC responses (coefficient of variation (CV): NGFCs: 15.6 ± 1.3%; FSBCs: 32.4 ± 2.7%), suggesting the possible involvement of more release sites (failure rates: NGFCs: 0%; FSBCs: 3.6 ± 1.3%). Furthermore, the connection probability was higher for NGFC–PC pairs recorded within

Author contributions: J.S., G.T., and I.S. designed research; J.S. and G.T. performed research; J.S. analyzed data; and J.S. and I.S. wrote the paper.

The authors declare no conflict of interest.

Freely available online through the PNAS open access option.

Abbreviations: FSBC, fast spiking basket cell; IPSC, inhibitory postsynaptic current; NGFC, neurogliaform cell; PC, pyramidal cell.

‡To whom correspondence should be addressed. E-mail: isoltesz@uci.edu.

This article contains supporting information online at www.pnas.org/cgi/content/full/0707204104/DC1.

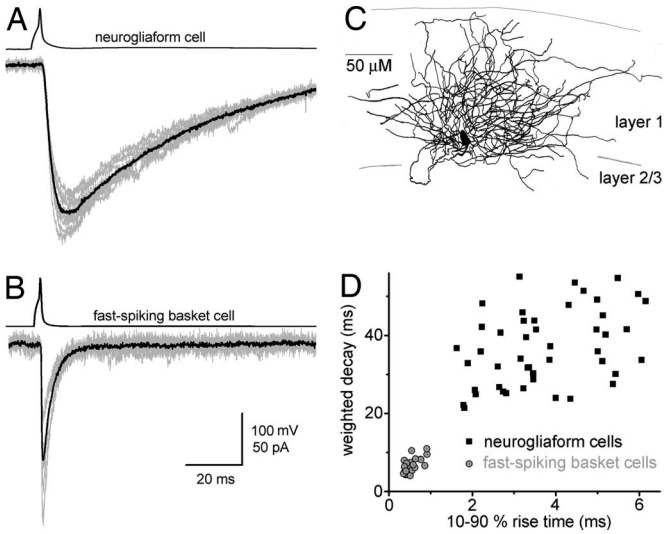

Fig. 1. Slow $GABA_A$ IPSCs evoked by NGFCs. (*A*) Ten consecutive $IPSC_A$s (gray, *Lower*) and their average (black) in a layer 2/3 PC after single action potentials in a layer 1 NGFC (*Upper*). (*B*) IPSCs evoked by a layer 2 FSBC. (*C*) Camera lucida reconstruction of the soma and axons of a NGFC from a 100-μm-thick section. Gray lines indicate the borders of cortical layers. (*D*) Comparison of the kinetics of postsynaptic responses evoked by NGFCs (black squares) and FSBCs (gray circles). Each point represents an individual connection.

≈100 μm, compared with FSBC–PC pairs (NGFC–PC pairs: 97.3%, 179 of 184; FSBC–PC pairs: 82.7%, 81 of 98). Finally, the synaptic delay of the NGFC–$IPSC_A$s (1.36 ± 0.11 ms) was also significantly longer compared with FSBC–$IPSC_A$s (0.5 ± 0.05 ms), but there was no difference in the CV of the onset delays (NGFCs: 16.2 ± 2.6%; FSBCs: 14.9 ± 2.1%).

Multiquantal, Asynchronous Release Cannot Explain the Slow Kinetics of the NGFC-Evoked $IPSC_A$s. What is the mechanism of the slow kinetics of the NGFC–$IPSC_A$? Although NGFCs innervate dendritic compartments of their postsynaptic targets (15, 16), dendritic filtering alone could not explain the extraordinarily slow rise- and decay kinetics of the NGFC-evoked events (*SI Methods 1* and SI Figs. 8 and 9). An alternative explanation for the slow kinetics may be related to the apparently higher number of release sites generating the NGFC–$IPSC_A$. It is possible that many asynchronous, fast quantal events underlie (17) the slow NGFC–$IPSC_A$ even after single spikes. To test this possibility, we compared the NGFC–$IPSC_A$s under conditions of low and high release probabilities, by repeatedly alternating between artificial cerebrospinal fluids (ACSFs) with either low (0.15 mM) or high (3 mM) Ca^{2+} concentrations (Fig. 2). As expected, the amplitude of the NGFC–$IPSC_A$s varied, by over an order of magnitude, as a function of the Ca^{2+} concentration in the ACSF. However, the extracellular Ca^{2+} concentration-induced large changes in event size had no discernible effect on the rise and decay kinetics of the NGFC–$IPSC_A$s (n = 4, Fig. 2), and the smallest events had a similarly slow rise and decay kinetics as the largest events. Therefore, the slow $GABA_A$ responses evoked by the NGFCs could not be primarily due to asynchronous release of presynaptic vesicles. These data also suggest that, although NGFC–$IPSC_A$s likely involve many release sites (see above), activation of a presumed single release site (as represented by the smallest discernable $IPSC_A$ in Fig. 2) generates responses that are similarly slow as the responses generated by multiple release sites.

Modulation of GABA Responses Evoked by NGFCs by GABA Uptake. It has been shown that hippocampal evoked $GABA_{A,fast}$ and

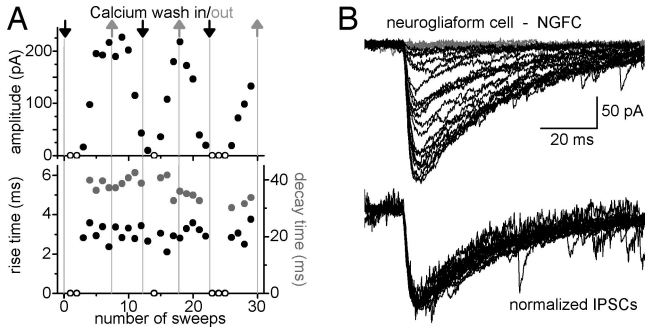

Fig. 2. Slow kinetics of NGFC–$IPSC_A$s are not due to multiquantal, asynchronous presynaptic vesicle release. (*A*) Rise times and decay time constants are independent from the amplitude of postsynaptic responses evoked by a NGFC. Arrows indicate the washing in of extracellular solutions with either low (0.15 mM, gray) or high (3 mM, black) calcium concentrations. Circles represent the amplitude (*Upper*, black), rise time (*Lower*, black) and decay time constant (gray) of individual events evoked by a NGFC. Open circles show where no postsynaptic responses could be detected. (*B*) Postsynaptic responses (*Upper*) obtained from a NGFC during the changing of the extracellular solutions with low or high Ca^{2+} concentrations. (*Lower*) Traces show the same responses after normalization.

$GABA_{A,slow}$ IPSCs displayed differential sensitivity to inhibition of GABA uptake (12). We tested whether a similar difference in the NGFC- and FSBC–$IPSC_A$s exists concerning modulation by NO711 (a specific blocker of GABA Transporter 1, GAT1; Fig. 3*A*). The decay of FSBC–$IPSC_A$s was not changed by 20 μM NO711 (14), whereas the NGFC–$IPSC_A$ became markedly pro-

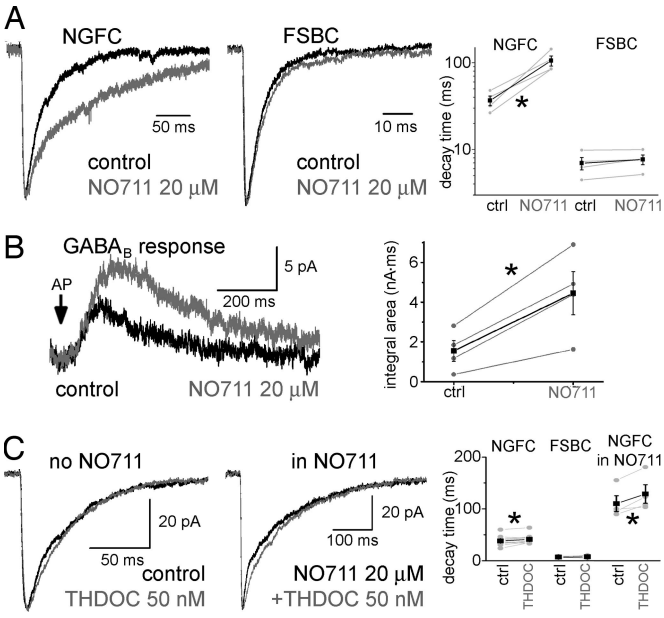

Fig. 3. Regulation by GABA uptake, and minor role for spillover in determining the slow kinetics of NGFC–$IPSC_A$s. (*A*) Averages of NGFC- (*Left*, n = 4) and FSBC–$IPSC_A$s (*Center*, n = 4) in control (black) and after application of 20 μM NO711 (gray). Note that the $IPSC_A$s were normalized to emphasize kinetic differences. Note also the different time scales. Summary data are shown (*Right*). Gray line plots show individual experiments. Black points represent the average results. Note the logarithmic scale. The asterisk marks significant difference. (*B*) Effect of 20 μM NO711 on NGFC-evoked $GABA_B$ responses (*Left*) (n = 4). Gray and black line plots represent the effects of NO711 on the integral area measured in individual experiments and their averages, respectively (*Right*). (*C*) Effect of 50 nM THDOC (gray) on NGFC–$IPSC_A$s without (*Left*, n = 11) and with NO711 present (20 μM, *Center*, n = 5). Summary data are shown (*Right*).

longed (τ_D; NGFC, pre-NO711: 36.6 ± 4.7 ms; NO711: 105.6 ± 13.9 ms; $n = 4$; FSBC pre-NO711: 6.9 ± 1.1 ms; NO711: 7.7 ± 1 ms, $n = 4$; the rise time of the responses did not change significantly: NGFC; before-NO711: 4.9 ± 1.3 ms; NO711: 4.2 ± 0.9 ms; FSBC; pre-NO711: 0.7 ± 0.08 ms; NO711: 0.72 ± 0.15 ms). Thus, these data were in good agreement with the previous observations concerning the differential NO711-sensitivity of spontaneous $GABA_{A,slow}$ and $GABA_{A,fast}$ events, supporting our hypothesis that $GABA_{A,slow}$ events were NGFC–$IPSC_A$s.

To better understand the NO711-sensitivity of the NGFC-evoked postsynaptic responses, we determined whether NO711 also enhances the $GABA_B$ IPSCs evoked by single NGFC spikes (15). Because postsynaptic $GABA_B$ receptors are located extrasynaptically (18–20), activation of these receptors by NGFCs suggested GABA spillover after single action potentials (15). The $GABA_B$ responses (recorded in the presence of 10 μM bicuculline without $GABA_B$ antagonist; for pipette solution, see *Materials and Methods*) evoked by single action potentials in NGFCs were strongly enhanced by NO711 (Fig. 3*B*; charge transfer pre-NO711: 1549 ± 519 pA·ms; NO711: 4459 ± 1089 pA·ms), indicating that GABA uptake markedly modulated both the $GABA_A$ and $GABA_B$ responses elicited by NGFCs.

Minor Role for High-Affinity $GABA_A$ Receptors in Determining the Slow Kinetics of the NGFC–$IPSC_A$s. The above data suggested that there was spillover of GABA from the synaptic cleft to the peri- and/or extrasynaptic space after single action potentials in NGFCs. However, it was not clear as to what extent this spillover contributed to the slow kinetics of the $GABA_A$ responses evoked by NGFCs. Therefore, in the next series of experiments, we assessed the activation of high-affinity, extrasynaptic $GABA_A$ receptors by NGFCs.

The δ-subunit is thought to be localized exclusively extrasynaptically (21, 22), and it is expressed by upper layer neocortical PCs (23). The δ subunit-specific positive modulator steroid, THDOC (50 nM) (7) slightly, but significantly, increased the τ_D of NGFC–$IPSC_A$s (Fig. 3*C*, pre-THDOC: 38.1 ± 2.6 ms; THDOC: 41.2 ± 2.4 ms; $n = 11$), without altering the amplitude (pre-THDOC: 60.6 ± 7.7 pA; THDOC: 60.8 ± 7.5 pA). The small effect of THDOC indicated that the slow kinetics of the NGFC–$IPSC_A$s did not originate as a result of high-affinity, δ-subunit-containing $GABA_A$ receptor activation (also note that, because of the small magnitude of the THDOC effect, the latter conclusion holds even if 50 nM THDOC partially acted on γ-subunit-containing receptors as well). As expected, FSBC–$IPSC_A$s were not affected by 50 nM THDOC (τ_D: pre-THDOC: 7.3 ± 0.8 ms; THDOC: 7.5 ± 1 ms; $n = 5$; amplitude: pre-THDOC: 49.8 ± 16.9 pA; THDOC: 50.6 ± 18.1 pA).

Even when GABA spillover was enhanced by application of NO711 (14), the effect of THDOC on the decay of the NGFC–$IPSC_A$s was still relatively small, albeit larger than without NO711 (Fig. 3*C*; τ_D: pre-THDOC: 110.1 ± 15.2 ms; THDOC: 128.7 ± 17.8 ms; $n = 4$; no change in amplitude: pre-THDOC: 84.1 ± 22.2 pA; THDOC: 86.5 ± 23.3 pA). THDOC significantly increased the holding current in the postsynaptic PCs (by 14 ± 6.9 pA), and this effect was more prominent in the presence of NO711 (69.6 ± 29 pA).

α5 subunits also form receptors with high affinity for GABA (8, 24), and they have been found both in the synaptic and extrasynaptic membranes of cortical cells (25). Therefore, we tested whether α5 subunit-containing receptors play a major role in shaping the uniquely slow kinetics of the NGFC–$IPSC_A$s. The α5 subunit-specific inverse agonist, L-655,708 (26) (10 μM) did not change the $IPSC_A$ decay (pre-L-655,708: 31.5 ± 3.9 ms; L-655,708: 31.9 ± 2.3 ms), but it had a moderate, although significant effect on the amplitude of NGFC–$IPSC_A$s (amplitude; pre-L-655,708: 127.4 ± 39.7 pA; L-655,708: 107.8 ± 34.1 pA; $n = 4$; data not shown).

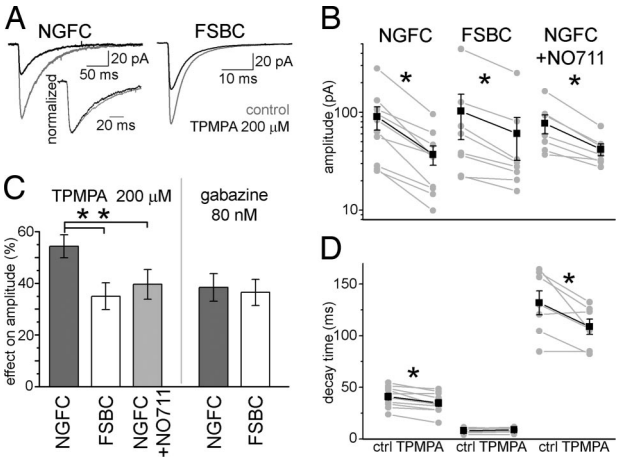

Fig. 4. Lower GABA concentration at the postsynaptic receptors in NGFC synapses compared with FSBC synapses. (*A*) Effect of 200 μM TPMPA (black) on NGFC- (*Left*) and FSBC–$IPSC_A$s (*Right*). Control $IPSC_A$s are shown in gray. (*Inset*) The normalized NGFC–$IPSC_A$s in control (gray) and TPMPA (black); note the acceleration of decay in TPMPA. (*B*) TPMPA effects on the peak amplitude in individual connections (gray). Black shows the average amplitude values in control and in presence of TPMPA. Asterisks mark significant differences. Note the logarithmic scale. (*C*) The relative blockade of different $IPSC_A$s (%) by 200 μM TPMPA and 80 nM gabazine. (*D*) Effects of TPMPA on the decay time constants in individual experiments (gray) and the average result (black).

Taken together, these results showed that high-affinity $GABA_A$ receptors were not the major determinants of the slow kinetics of the $GABA_A$ responses evoked by NGFCs.

Low GABA Concentration at Postsynaptic $GABA_A$ Receptors After GABA Release from NGFCs. The GABA-transient is likely to be a major factor in determining the properties of GABA responses (27). To compare the transmitter concentration at the postsynaptic receptors in NGFC and FSBC synapses, we measured the effect of a low-affinity, competitive $GABA_A$ receptor antagonist, TPMPA, on the $IPSC_A$s generated by these two interneuron subtypes (28–30). The effect of TPMPA (200 μM) was significantly larger (with both *t* tests and the nonparametric Mann–Whitney test) on the amplitude of NGFC–$IPSC_A$s (Fig. 4 *A–C*, pre-TPMPA: 89.8 ± 24 pA; TPMPA: 37 ± 8.3 pA; effect: 54.3 ± 4.5%; $n = 10$) compared with the FSBC–$IPSC_A$s (pre-TPMPA: 102.6 ± 50 pA; TPMPA: 60.5 ± 28.2 pA; effect: 35 ± 5.2%; $n = 8$), indicating significantly lower GABA concentration at the postsynaptic receptors at NGFC synapses compared with FSBC synapses. After blockade of GABA uptake with 20 μM NO711, TPMPA had significantly less effect on the amplitude of NGFC–$IPSC_A$s (Fig. 4 *B* and *C*; pre-TPMPA: 77 ± 17 pA; TPMPA: 41.8 ± 5.7 pA; effect: 39.6 ± 5.7%; $n = 7$) than without NO711. In contrast to TPMPA, the high-affinity, competitive antagonist gabazine at low concentration (80 nM) decreased the two types of $IPSC_A$s similarly (Fig. 4*C*; NGFC: pregabazine: 36.8 ± 8 pA; gabazine: 22.4 ± 3.9 pA; effect: 36.5 ± 5.1%; $n = 4$; FSBC: pregabazine: 57.5 ± 14 pA; gabazine: 36.2 ± 10.2 pA; effect: 38.4.2 ± 5.4%; $n = 5$).

Furthermore, NGFC–$IPSC_A$s had a significantly faster decay in presence of TPMPA (34.9 ± 3.1 ms) than before TPMPA was applied (41 ± 3.1 ms; effect: −15.4 ± 3.5%) (Fig. 4 *A* and *D*). The TPMPA-effect on the NGFC–$IPSC_A$ decay persisted when TPMPA was applied in the presence of NO711 (pre-TPMPA: 131.6 ± 11.6 ms; TPMPA: 108.6 ± 7.5 ms; effect: −15.7 ± 5%). In contrast, the kinetics of FSBC–$IPSC_A$s were not changed (pre-TPMPA: 8.55 ± 0.87 ms; TPMPA: 8.79 ± 0.79 ms). The sensitivity of the decay phase of the NGFC–$IPSC_A$ to the

NEUROSCIENCE

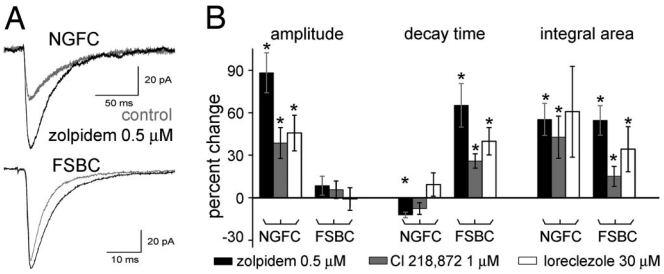

Fig. 5. Role of low-affinity $GABA_A$ receptors in NGFC- and FSBC–$IPSC_A$s. (*A*) Effect of zolpidem (black) on $GABA_A$ responses evoked by NGFCs (*Upper*) and FSBCs (*Lower*). Control traces are shown in gray. Traces show the average of seven and five experiments, respectively. (*B*) Effects of zolpidem (black), Cl218,872 (gray), and loreclezole (white) on the properties of NGFC- and FSBC–$IPSC_A$s relative to control. Asterisks mark significant differences with respect to predrug conditions.

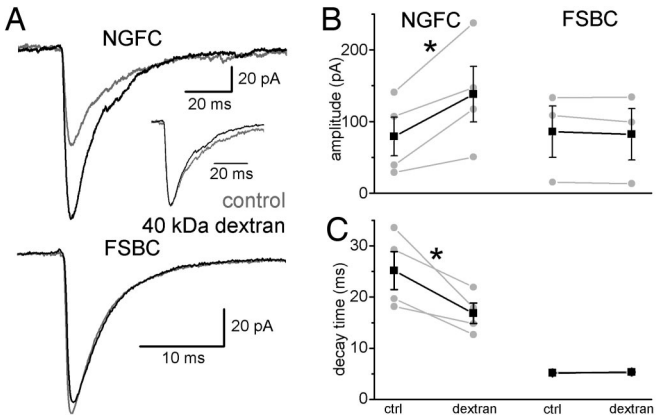

Fig. 6. Slowing diffusion alters NGFC–$IPSC_A$s but not FSBC–$IPSC_A$s. (*A*) Effects of dextran (black) on NGFC- (*Upper*) and FSBC–$IPSC_A$s (*Lower*). Control $IPSC_A$s are shown in gray. (*Inset*) Normalized NGFC–$IPSC_A$s in control (gray) and dextran (black). Note the faster decay in dextran. (*B*) Changes of peak amplitudes in individual connections (gray) and average (black) after perfusion of dextran. Asterisk marks significant difference. (*C*) Effects of dextran on the decay time constants in individual experiments (gray) and the average result (black).

low-affinity competitive antagonist is consistent with the presence of spillover (14).

Low-Affinity $GABA_A$ Receptors Underlying the NGFC- and FSBC–$IPSC_A$s. Next, we used positive $GABA_A$ receptor modulators with subunit specificity to study the contribution of the low-affinity $GABA_A$ receptors to the generation of the NGFC–$IPSC_A$s. Zolpidem, like other benzodiazepines, increases the affinity of the receptors to GABA and increase the open probability of $GABA_A$ channels when GABA is present (31, 32). It preferentially acts on $GABA_A$ receptors containing the $\alpha 1$ subunit and, to a lesser extent, on receptors with $\alpha 2/\alpha 3$ subunits (33, 34). The most dramatic effect of zolpidem (0.5 μM) was that it increased the amplitude of NGFC–$IPSC_A$s (Fig. 5; prezolpidem: 43.4 ± 6.7 pA; zolpidem: 82 ± 14 pA; $n = 7$), whereas it did not significantly change the amplitude of FSBC–$IPSC_A$s (prezolpidem: 78.5 ± 25.6ms; zolpidem: 81.6 ± 24.9 pA; $n = 5$). As expected, zolpidem robustly prolonged the decay of the FSBC–$IPSC_A$s (Fig. 5; prezolpidem: 6.1 ± 0.6 ms; zolpidem: 10.7 ± 2.1 ms), whereas it did not prolong the decay of the NGFC–$IPSC_A$s (prezolpidem: 37.6 ± 2.1 ms; zolpidem: 33.0 ± 2 ms; note that the latter change represented a small (12.1 ± 1.9%), but significant acceleration of the NGFC–$IPSC_A$ decay by zolpidem).

Next, we used Cl218,872, which displays a greater selectivity for $GABA_A$ receptors containing the $\alpha 1$ subunit than zolpidem (33). In agreement with the reported higher affinity of Cl218,872 to $\alpha 1\beta x\gamma 2$ receptors, in control experiments, we verified that the axo-axonic cell-evoked $IPSC_A$s, which are known to be mediated through $\alpha 2$ subunit-containing receptors (35), were not affected by Cl218,872 ($n = 2$, data not shown). Cl218,872 (1 μM) had potent enhancing effects on the amplitude of NGFC–$IPSC_A$s (Fig. 5*B*; pre-Cl218,872: 95.8 ± 18.8 pA; Cl218,872: 134.6 ± 30.9 pA; $n = 6$), without altering the FSBC–$IPSC_A$ amplitude (pre-Cl218,872: 113 ± 66.7 pA; Cl218,872: 112.9 ± 62.7 pA; $n = 5$). Like zolpidem, Cl218,872 significantly increased the decay of the FSBC–$IPSC_A$s (pre-Cl218,872: 6.1 ± 1.5 ms; Cl218,872: 8 ± 2.4 ms), and it did not prolong NGFC–$IPSC_A$s (pre-Cl218,872: 38.5 ± 1.6 ms; Cl218,872: 35.3 ± 0.7 ms; note that there was actually a slight (7.7 ± 4.1%), but nonsignificant, acceleration of the decay). Cl218,872 also acted similarly to zolpidem on the overall charge transfers.

Next, we tested the effects of loreclezole, a positive modulator of $\beta 2$- or $\beta 3$-containing $GABA_A$ receptors (33). Similar to zolpidem and Cl218,872, loreclezole (30 μM) enhanced the amplitude of the NGFC–$IPSC_A$s (Fig. 5*B*; preloreclezole: 54.1 ± 22.7 pA; loreclezole: 73.3 ± 27.3 pA; $n = 5$), without affecting the FSBC–$IPSC_A$ amplitude (preloreclezole: 117.2 ± 59.9 pA; loreclezole: 111.4 ± 53 pA; $n = 4$). Furthermore, loreclezole significantly prolonged the decay of the FSBC–$IPSC_A$s (preloreclezole: 5.1 ± 0.8 ms; loreclezole: 7 ± 0.8 ms), but not the NGFC–$IPSC_A$s (preloreclezole: 40.2 ± 4.7 ms; loreclezole: 43.8 ± 6 ms).

As a positive control, we showed that zolpidem was able to increase the amplitude of FSBC–$IPSC_A$s at room temperature (31) (*SI Methods 2* and SI Fig. 10). We also determined that differential zolpidem effects on NGFC- and FSBC–$IPSC_A$s were not due to a presynaptic action leading to a potentiation of GABA release from NGFCs (*SI Methods 3* and SI Fig. 11). In addition, experiments with presynaptically applied bafilomycin revealed that low vesicular GABA concentration is unlikely to underlie the slow kinetics of the NGFC–$IPSC_A$ (*SI Methods 4* and SI Fig. 12; note that we directly verified that bafilomycin did, in fact, decrease the synaptic GABA concentration at FSBC synapses, because TPMPA had a significantly larger effect in the presence of bafilomycin).

Taken together, these data suggested that $\alpha 1$, $\beta 2/3$, and $\gamma 2$ subunit-containing low-affinity $GABA_A$ receptors were the most likely to play a dominant role in mediating the responses evoked by both NGFCs and FSBCs. Because $\alpha 1\beta 2/3\gamma 2$ receptors are the major synaptic $GABA_A$ receptors in the neocortex (33, 34), these data were in agreement with our results indicating that high-affinity $GABA_A$ receptors had only a minor contribution to the generation of NGFC-derived $GABA_A$ responses. The amplitude-enhancing effect of benzodiazepines is usually interpreted to indicate lack of saturation of the receptors (31), and it is thus consistent with the TPMPA-results described above, indicating lower concentration of GABA at the postsynaptic receptors after GABA release from NGFCs.

Slowing Diffusion Affects NGFC–$IPSC_A$s but Not FSBC–$IPSC_A$s. To further study the mechanism of the slow NGFC–$IPSC_A$-s, we slowed GABA diffusion by adding 1.25 mM (5% wt/vol) of the inert macromolecule dextran (MW: 40,000 g) to the extracellular medium (27, 29, 36) while recording NGFC–$IPSC_A$s or FSBC–$IPSC_A$s. Dextran significantly increased the amplitude of NGFC–$IPSC_A$s (Fig. 6; predextran: 79 ± 27 pA; dextran: 138.2 ± 38.9 pA; $n = 4$), but it did not change the amplitude of FSBC–$IPSC_A$s (predextran: 85.7 ± 35.9 pA; dextran: 82.1 ± 36 pA; $n = 3$). Furthermore, dextran significantly decreased the decay time constant of NGFC–$IPSC_A$s (τ_D: predextran: 25.2 ± 3.7 ms; dextran: 16.8 ± 2ms), but not the τ_D of FSBC–$IPSC_A$s

(predextran: 5.2 ± 0.1 ms; dextran: 5.3 ± 0.1 ms). The dextran-induced enhancement of amplitude and acceleration of decay of the NGFC–IPSC$_A$s are consistent with an increased intracleft GABA concentration and decreased activation of extrasynaptic receptors resulting from less GABA escaping from the synapse into the extrasynaptic space in the presence of slowed diffusion.

Discussion

Cellular Origin of GABA$_{A,slow}$ Events. Specialized classes of cortical GABA cells exert complex effects on PC activity, including regulation of excitatory postsynaptic potential integration, modulation of dendritic plasticity, and synchronization of neuronal ensembles. A critically important factor in the GABAergic regulation of principal cell function is the time course of inhibitory inputs. The present results revealed striking similarities between previously described spontaneous and evoked GABA$_{A,slow}$ events (10–13, 37) and NGFC–IPSC$_A$s, including (*i*) extraordinarily slow rise and decay kinetics; (*ii*) charge transfer that is considerably larger than in FSBC–IPSCs; (*iii*) special sensitivity to GAT1 blockade; and (*iv*) enhancement of amplitudes by bath-applied benzodiazepines (13). Based on these similarities, we conclude that GABA$_{A,slow}$ IPSCs originate from NGFCs.

GABA Spillover at NGFC Synapses. The presence of spillover at NGFC synapses was suggested by several lines of evidence. First, uniquely among all known GABAergic interneurons, single presynaptic action potentials of NGFCs can activate postsynaptic GABA$_B$ receptors (15), which are localized extrasynaptically (18–20, 38). Second, as shown in our experiments, transport blockade dramatically increased the activation of GABA$_B$ receptors. Third, THDOC had a significant effect on the decay of NGFC–IPSC$_A$s even without GAT1 blockade. Because the THDOC-sensitive, high-affinity, δ-subunit-containing GABA$_A$ receptors are peri- and extrasynaptically localized (7, 21, 22), the THDOC-induced prolongation of the IPSC decay was consistent with the presence of spillover. Fourth, the THDOC-effect on the NGFC–IPSC$_A$ decay was increased by NO711. Fifth, NGFC–IPSC$_A$ decays were accelerated by TPMPA even in the absence of NO711 (14, 39, 40). Sixth, the decay of NGFC–IPSC$_A$s became faster when diffusion was limited by dextran (27, 29, 36), which was also consistent with spillover. It is interesting to note that, because of the presence of spillover, NGFCs may contribute to the regulation of the ambient level of GABA (41–43).

Nature of the Transmitter Transient at NGFC Synapses. Although the data suggested GABA spillover at NGFC synapses, spillover alone could not have explained the extreme slowness of the NGFC–IPSC$_A$s. First, THDOC prolonged the NGFC–IPSC$_A$ decay to only a small extent. Second, even after transporter blockade, the contribution of the high-affinity GABA$_A$ receptors to the overall NGFC–IPSC$_A$ was minor. In contrast, a major factor underlying the unique properties of the NGFC–IPSC$_A$s appeared to be the nature of the GABA transient. A key observation in this regard was that the low-affinity, competitive GABA$_A$ receptor antagonist TPMPA had a significantly larger inhibitory effect on the peak amplitude of the NGFC–IPSC$_A$s than on the FSBC–IPSC$_A$s. These data indicated that the peak transmitter concentration in the vicinity of the postsynaptic receptors during GABA transients after single action potentials in NGFCs was smaller than after GABA release from FSBCs. However, the amplitude of the NGFC–IPSC$_A$s was dramatically increased under conditions of slowed diffusion, an effect that could be explained by the entrapment of GABA within the synaptic cleft by the dextran (note that dextran did not affect the FSBC–IPSC$_A$s, indicating that the macromolecule stayed primarily in the extrasynaptic space and did not enter the synaptic cleft to slow down diffusion). Our experiments demonstrated that GAT1 was important in setting the lower peak GABA concentration during the NGFC-evoked GABA transients, because TPMPA had a significantly smaller effect on the NGFC–IPSC$_A$ amplitude when GABA uptake was inhibited.

The nature of the GABA transient at NGFC synapses could be probed by using benzodiazepines, because previous studies suggested that benzodiazepines such as zolpidem enhance IPSC amplitudes under conditions of submaximal saturation of GABA$_A$ receptors and/or asynchronous receptor activation (31, 32). Our results revealed that, at physiological temperature, zolpidem enhanced the amplitude of the NGFC–IPSC$_A$s but prolonged the decay of the FSBC–IPSC$_A$s. Furthermore, two other drugs with distinct subunit preference had similar effects on the NGFC–IPSC$_A$ amplitudes. The amplitude-enhancing effect of the various positive GABA$_A$ receptor modulators is consistent with a slowly rising GABA transient with low peak GABA concentration at NGFC synapses.

Although nonsaturating GABA puffs have been shown to slow current kinetics (31, 44), low peak GABA concentration alone did not appear to be sufficient to explain the slow kinetics, because lowering of the GABA concentration at FSBC synapses did not result in NGFC–IPSC$_A$-like slow kinetics (*SI Methods 4* and SI Fig. 12). A potentially significant factor in generating the slow responses may be related to the structural features of NGFC synapses. Indeed, these synapses are small (in terms of the junctional area) relative to other synapses (15, 16, 38), and it is interesting that many of our observations could be explained if the small NGFC synapses contained a larger cleft distance between the pre- to postsynaptic synapse membranes. The larger cleft distance would be expected to result in a slower rising transient with a lower peak GABA concentration at the postsynaptic membranes, because GABA would be diluted in the larger cleft space. Furthermore, the small junctional area and the large cleft distance would facilitate spillover, because GABA could preferentially escape to the extrasynaptic space from the more open edges surrounding the shorter but wider cleft. Because *in vitro* biocytin-filled materials are not appropriate for the precise measurement of the cleft size (see SI Fig. 8), carefully designed quantitative electron microscopic studies will need to be carried out to determine the microstructure of NGFC synapses. Additional factors, such as the potentially prolonged nature of the GABA transient, perhaps related to special kinetic properties of the synaptic release machinery in NGFC terminals, may also play a role in contributing to the slowness of the NGFC–IPSC$_A$s.

The present results demonstrate that a single action potential in the presynaptic NGFCs is able to evoke slow IPSC$_A$s. The latter point is important, because it is known that repetitive stimulation can prolong the decay of unitary IPSC$_A$s (14). Although NGFC–IPSC$_A$s seem to involve a relatively large number of release sites, activation of many release sites is not necessary for generating the characteristically slow kinetics. Furthermore, the compact and dense axonal cloud enables NGFCs to be connected to virtually every neighboring pyramidal and GABAergic cell (15, 38, 45–47). NGFCs receive extensive local and ascending excitatory drive (38, 46, 48), and they can detect the activity of other types of interneurons through a nonspecific gap junctional network (38, 46, 47). Therefore, NGFCs may monitor the activity of a large set of neurons in cortical networks and provide powerful inhibition to a spatially restricted group of neurons through prolonged GABA$_A$ and GABA$_B$ receptor-mediated events.

Materials and Methods

All protocols were approved by the Institutional Animal Care and Use Committee of the University of California.

Electrophysiology. Slices (320 μm) were prepared from 20- to 26-day-old Wistar rats in ice-cold artificial cerebrospinal fluid

(85 mM NaCl, 75 mM sucrose, 2.5 mM KCl, 25 mM glucose, 1.25 mM NaH_2PO_4, 4 mM $MgCl_2$, 0.5 mM $CaCl_2$, and 24 mM $NaHCO_3$). Before the recording session, the slices were kept at room temperature. Slices were visualized by using an upright microscope (Eclipse FN-1; Nikon, East Rutherford, NJ) with infrared differential interference contrast optics. Presynaptic interneurons in the somatosensory cortex were recorded in current clamp mode [intracellular solution: 126 mM potassium gluconate, 4 mM KCl, 10 mM Hepes, 4 mM ATP-Mg, 0.3 mM GTP-Na, 10 mM phosphocreatine, and 8 mM biocytin (pH 7.2), 270–290 mOsm] and held at −60mV. Short (2.5-ms) current injections were delivered to evoke single action potentials. The postsynaptic cells were layer 2/3 PCs, held at −75 mV by using MultiClamp 700B amplifier (Molecular Devices, Union City, CA). Postsynaptic intracellular solution was typically composed of 40 mM CsCl, 90 mM potassium gluconate, 1.8 mM NaCl, 1.7 mM $MgCl_2$, 3.5 mM KCl, 0.05 mM EGTA, 10 mM Hepes, 2 mM Mg-ATP, 0.4 mM Na_2-GTP, and 10 mM phosphocreatine (pH 7.2); 270–290 mOsm; for $GABA_B$ responses, the intracellular solution was 110 mM potassium gluconate, 1.8 mM NaCl, 1.7 mM $MgCl_2$, 23.5 mM KCl, 0.05 mM EGTA, 10 mM Hepes, 2 mM Mg-ATP, 0.4 mM Na_2-GTP, and 10 mM phosphocreatine. As described before, the transmission from NGFCs is highly sensitive to the firing of presynaptic cells (15). Therefore, to avoid accidental overexcitation of presynaptic cells during patch formation, we used an extracellular solution with low Ca^{2+} (0.15 mM) to establish whole-cell recordings. Once stable recordings were obtained from the interneuron and the PC, the low-Ca^{2+} extracellular solution was changed to normal perfusate, revealing the presence or absence of synaptic connections between the two neurons. Unless mentioned otherwise, normal recording solution was composed of 126 mM NaCl, 2.5 mM KCl, 26 mM $NaHCO_3$, 2 mM $CaCl_2$, 2 mM $MgCl_2$, 1.25 mM NaH_2PO_4, 10 mM glucose, 0.02 mM d-AP-5, 0.005 mM NBQX, and 0.00025 mM CGP55845. All electrophysiological recordings were made at 36°C. Presynaptic interneurons were identified based on their firing properties and axonal morphologies (SI Fig. 7 and Fig. 1*C*) (15, 45). Series resistances were continuously monitored, and the recordings were discarded if the series resistance changed ±30% or reached 20 MΩ. The decay of IPSCs was fitted with two exponentials. Drugs were dissolved and stored according to the manufacturer's instructions and were bath-applied. Values are shown as mean and SEM. Paired or independent *t* test (two-tailed) were used for statistical analysis ($P < 0.05$) (in addition, as indicated, the nonparametric Mann–Whitney test was also used in certain cases). Traces in figures usually show the average of all experiments for any given treatment.

Anatomy. Slices were transferred into a fixative solution containing 4% paraformaldehyde and 0.2% picric acid in 0.1 M phosphate buffer after the recording for 2–4 days, then resectioned at 100 μm. ABC reaction (Vectastain ABC Kit; Vector Laboratories, Burlingame, CA) was done overnight, and then slices were reacted with DAB (Vector Laboratories) for 15 min. Sections were mounted on glass slides, dehydrated with a five-step ethanol series, and mounted with DPX mounting media (EMS, Fort Washington, PA).

We thank Ms. R. Zhu for expert technical assistance and Dr. S. Ross for the generous loan of a Nikon FN-1 Eclipse microscope. This work was funded by a National Institutes of Health Grant NS35915 (to I.S. and G.T.), the Wellcome Trust, the Hungarian Academy of Sciences, the National Office for Research and Technology (NKTH) Polányi Award, Hungarian Scientific Research Fund (OTKA) Grant T049535, Howard Hughes Medical Institute Grant 55005625 and a European Young Investigator (EURYI) Award (to G.T.), the Boehringer Ingelheim Fonds, and the George E. Hewitt Foundation for Medical Research (to J.S.).

1. Mody I, Pearce RA (2004) *Trends Neurosci* 27:569–575.
2. Semyanov A, Walker MC, Kullmann DM, Silver RA (2004) *Trends Neurosci* 27:262–269.
3. Kullmann DM, Ruiz A, Rusakov DM, Scott R, Semyanov A, Walker MC (2005) *Prog Biophys Mol Biol* 87:33–46.
4. Farrant M, Nusser Z (2005) *Nat Rev Neurosci* 6:215–229.
5. Jonas P, Bischofberger J, Fricker D, Miles R (2004) *Trends Neurosci* 27:30–40.
6. Brickley SG, Cull-Candy SG, Farrant M (1996) *J Physiol* 497(Pt 3):753–759.
7. Stell BM, Brickley SG, Tang CY, Farrant M, Mody I (2003) *Proc Natl Acad Sci USA* 100:14439–14444.
8. Hamann M, Rossi DJ, Attwell D (2002) *Neuron* 33:625–633.
9. Mitchell SJ, Silver RA (2003) *Neuron* 38:433–445.
10. Pearce RA (1993) *Neuron* 10:189–200.
11. Banks MI, Li TB, Pearce RA (1998) *J Neurosci* 18:1305–1317.
12. Banks MI, White JA, Pearce RA (2000) *Neuron* 25:449–457.
13. Prenosil GA, Schneider Gasser EM, Rudolph U, Keist R, Fritschy JM, Vogt KE (2006) *J Neurophysiol* 96:846–857.
14. Overstreet LS, Westbrook GL (2003) *J Neurosci* 23:2618–2626.
15. Tamas G, Lorincz A, Simon A, Szabadics J (2003) *Science* 299:1902–1905.
16. Vida I, Halasy K, Szinyei C, Somogyi P, Buhl EH (1998) *J Physiol* 506(Pt 3):755–773.
17. Hefft S, Jonas P (2005) *Nat Neurosci* 8:1319–1328.
18. Scanziani M (2000) *Neuron* 25:673–681.
19. Kulik A, Vida I, Lujan R, Haas CA, Lopez-Bendito G, Shigemoto R, Frotscher M (2003) *J Neurosci* 23:11026–11035.
20. Vigot R, Barbieri S, Brauner-Osborne H, Turecek R, Shigemoto R, Zhang YP, Lujan R, Jacobson LH, Biermann B, Fritschy JM, *et al.* (2006) *Neuron* 50:589–601.
21. Nusser Z, Sieghart W, Somogyi P (1998) *J Neurosci* 18:1693–1703.
22. Wei W, Zhang N, Peng Z, Houser CR, Mody I (2003) *J Neurosci* 23:10650–10661.
23. Drasbek KR, Jensen K (2006) *Cereb Cortex* 16:1134–1141.
24. Caraiscos VB, Elliott EM, You-Ten KE, Cheng VY, Belelli D, Newell JG, Jackson MF, Lambert JJ, Rosahl TW, Wafford KA, *et al.* (2004) *Proc Natl Acad Sci USA* 101:3662–3667.
25. Serwanski DR, Miralles CP, Christie SB, Mehta AK, Li X, De Blas AL (2006) *J Comp Neurol* 499:458–470.
26. Quirk K, Blurton P, Fletcher S, Leeson P, Tang F, Mellilo D, Ragan CI, McKernan RM (1996) *Neuropharmacology* 35:1331–1335.
27. Nielsen TA, DiGregorio DA, Silver RA (2004) *Neuron* 42:757–771.
28. Jones MV, Jonas P, Sahara Y, Westbrook GL (2001) *Biophys J* 81:2660–2670.
29. Barberis A, Petrini EM, Cherubini E (2004) *Eur J Neurosci* 20:1803–1810.
30. Barberis A, Lu C, Vicini S, Mozrzymas JW (2005) *Mol Pharmacol* 67:1221–1228.
31. Perrais D, Ropert N (1999) *J Neurosci* 19:578–588.
32. Baur R, Sigel E (2005) *Mol Pharmacol* 67:1005–1008.
33. Korpi ER, Grunder G, Luddens H (2002) *Prog Neurobiol* 67:113–159.
34. Mohler H (2006) *Cell Tissue Res* 326:505–516.
35. Nusser Z, Sieghart W, Benke D, Fritschy JM, Somogyi P (1996) *Proc Natl Acad Sci USA* 93:11939–11944.
36. Min MY, Rusakov DA, Kullmann DM (1998) *Neuron* 21:561–570.
37. Glykys J, Mody I (2006) *J Neurophysiol* 95:2796–2807.
38. Price CJ, Cauli B, Kovacs ER, Kulik A, Lambolez B, Shigemoto R, Capogna M (2005) *J Neurosci* 25:6775–6786.
39. Carter AG, Regehr WG (2000) *J Neurosci* 20:4423–4434.
40. Diamond JS (2001) *J Neurosci* 21:8328–8338.
41. Jensen K, Chiu CS, Sokolova I, Lester HA, Mody I (2003) *J Neurophysiol* 90:2690–2701.
42. Richerson GB, Wu Y (2003) *J Neurophysiol* 90:1363–1374.
43. Scimemi A, Semyanov A, Sperk G, Kullmann DM, Walker MC (2005) *J Neurosci* 25:10016–10024.
44. Jones MV, Westbrook GL (1995) *Neuron* 15:181–191.
45. Karube F, Kubota Y, Kawaguchi Y (2004) *J Neurosci* 24:2853–2865.
46. Chu Z, Galarreta M, Hestrin S (2003) *J Neurosci* 23:96–102.
47. Simon A, Olah S, Molnar G, Szabadics J, Tamas G (2005) *J Neurosci* 25:6278–6285.
48. Zhu Y, Zhu JJ (2004) *J Neurosci* 24:1272–1279.